The radical SAM protein HemW is a heme chaperone

Vera Haskamp, Simone Karrie, Toni Mingers, Stefan Barthels, François Alberge, Axel Magalon, Katrin Müller, Eckhard Bill, Wolfgang Lubitz, Kirstin Kleeberg, et al.

The radical SAM protein HemW is a Heme Chaperone

Vera Haskamp[1], Simone Karrie[1,], Toni Mingers[1], Stefan Barthels[1], François Alberge[2], Axel Magalon[2], Katrin Müller[1], Eckhard Bill[3], Wolfgang Lubitz[3], Kirstin Kleeberg[4], Peter Schweyen[4], Martin Bröring[4], Martina Jahn[1] and Dieter Jahn[5]

[1]Institute of Microbiology, University Braunschweig, Braunschweig, Germany,[2]LCB, CNRS, Aix-Marseille Université, Marseille, France,[3]Max Planck Institute for Chemical Energy Conversion, Mülheim an der Ruhr, Germany,[4]Institute of Inorganic and Analytical Chemistry, University Braunschweig, Braunschweig, Germany,[5]Braunschweig Centre of Integrated Systems Biology (BRICS), University Braunschweig, Braunschweig, Germany

Running title: Novel Heme Chaperone HemW

To whom correspondence should be addressed: Dieter Jahn, Braunschweig Centre of Integrated Systems Biology (BRICS), University Braunschweig, Rebenring 56, D-38106 Braunschweig, Germany. Tel.: +4953139155101, E-mail: d.jahn@tu-bs.de

Keywords: HemW, heme chaperone, radical SAM, iron-sulfur cluster, *Escherichia coli*

ABSTRACT

Radical *S*-adenosylmethionine (SAM) enzymes exist in organisms from all kingdoms of life, and all of these proteins generate an adenosyl radical via the homolytic cleavage of the S–C(5') bond of SAM. Of particular interest are radical SAM enzymes, such as heme chaperones, that insert heme into respiratory enzymes. For example, heme chaperones insert heme into target proteins, but have been studied only for the formation of cytochrome *c* type hemoproteins. Here, we report that a radical SAM protein, the heme chaperone HemW from bacteria, is required for the insertion of heme *b* into respiratory chain enzymes. As other radical SAM proteins, HemW contains three cysteines and one SAM coordinating an [4Fe-4S] cluster, and we observed one heme per subunit of HemW. We found that an intact iron-sulfur cluster was required for HemW dimerization and HemW-catalyzed heme transfer, but not for stable heme binding. A bacterial two-hybrid system screen identified bacterioferritins and the heme-containing subunit NarI of the respiratory nitrate reductase NarGHI as proteins that interact with HemW. We also noted that the bacterioferritins potentially serve as heme donors for HemW. Of note, heme that was covalently bound to HemW was actively transferred to a heme-depleted, catalytically inactive nitrate reductase, restoring its nitrate-reducing enzyme activity. Finally, the human HemW orthologue radical SAM domain–containing 1 (RSAD1) stably bound heme. In conclusion, our findings indicate that the radical SAM protein family HemW/RSAD1 is a heme chaperone catalyzing the insertion of heme into hemoproteins.

Radical SAM enzymes have been discovered in organisms from all kingdoms of life (1-3). The currently known 114.000

radical SAM proteins catalyze a broad variety of challenging chemical reactions (4-7). For instance, humans possess eight radical SAM proteins: 1. MOCS1 involved in molybdenum cofactor biosynthesis, 2. LIAS for the formation of lipoic acid, 3. CDK5RAP for 12-methylthio-N(5)-isopentenyladenosine synthesis, 4. CDKAL1 required for methylthio-N(6)-threonylcarbamoyladenosine formation, 5. TYW1 for wybutosine biosynthesis, 6. ELP3 for 5-methoxycarbonymethyl uridine, 7. Viperin and 8. RSAD1, respectively (reviewed in (2). Viperin is involved in the innate antiviral response (8). However, the exact enzymatic function of human viperin and RSAD1 are currently unknown.

All have in common the generation of a adenosyl radical via the homolytic cleavage of the S–C(5') bond of SAM. SAM and three cysteine residues generally coordinate a [4Fe-4S] cluster, leading to the typical CX_3CX_2C protein sequence signature of radical SAM enzymes (1). The first crystal structure of a radical SAM enzyme was solved for an enzyme of bacterial heme biosynthesis called coproporphyrinogen III dehydrogenase (HemN) (9). Three iron atoms of the [4Fe-4S] cluster of HemN are coordinated by the three cysteine residues Cys^{62}, Cys^{66} and Cys^{69} of the conserved motif (9,10). A fourth cysteine (Cys^{71}) is not essential for [4Fe-4S] cluster coordination, but for catalysis (10). During the catalytic reaction for the conversion of coproporphyrinogen III into protoporphyrinogen IX the $[4Fe\text{-}4S]^{2+}$ cluster first gets reduced. This leads to the homolytic cleavage of the SAM S-C(5') bond and the formation of a 5'-deoxyadenosyl radical. The generated radical then removes stereospecifically one hydrogen atom from a propionate side chain of the substrate to yield 5'-deoxyadenosine and a substrate radical which in turn leads to the desired decarboxylation reaction (9,11). However, the presence of HemN proteins (also named CPDH) carrying the CX_3CX_2CXC motif is limited to a few classes of bacteria (12). Multiple *hemN*-like genes encoding proteins of significant amino acid sequence homology were found in most classes of organisms with the exception of fungi and were originally annotated as coproporphyrinogen III oxidase.

Recently, the corresponding *Lactococccus lactis* protein *w*as observed to bind heme and considered to play a role in maturation of the cytochrome oxidoreductase of the bacterium. It was therefore renamed HemW (13). *L. lactis* HemW (NP_267295.1) displays high homology to *Escherichia coli* coproporphyrinogen III dehydrogenase HemN (50 % amino acid sequence similarity). Surprisingly, *L. lactis* HemW did not show CPDH activity *in vitro* and *in vivo (13)*. In contrast to *E. coli* HemN, *L. lactis* HemW is missing 47 N-terminal amino acids and the fourth cysteine residue of the conserved CX_3CX_2CXC motif (13). *E. coli* possesses HemN and additionally a HemW-like protein annotated as YggW (NP_417430.1), a protein of hypothetical function. Because of the high degree of amino acid sequence identity of 36% (58% homology) to *L. lactis* HemW we renamed YggW to HemW in the present work. Relatedly, the corresponding *Pseudomonas aeruginosa* protein (WP_003128950) with an amino acid sequence identity of 31% (50% homology) to *L. lactis* HemW was also renamed to HemW. Similar to *L. lactis* HemW, the HemWs of *E. coli* and *P. aeruginosa* displayed a truncated N-terminus and the conserved cysteine motif lacking the fourth cysteine. A corresponding amino acid sequence alignment is shown in figure S1.

The only well characterized systems for the insertion of heme into proteins are the different cytochrome *c* biogenesis machine ries (14). Cytochrome *c* is involved in multiple electron transport chains. For cytochrome *c* formation rotoheme IX and the apocytochrome are transported through

the membranes of prokaryotes, mitochondria and chloroplasts. Subsequently, a covalent thioether bond is actively formed between at least one cysteine and a vinyl group of the heme. Currently, 5 different systems are proposed to perform the processes of heme insertion into a *c*-type cytochrome which differ in their level of complexity and are found in distinct organisms (14). Sporadically, reports on other heme binding and potential heme inserting proteins occur in the literature, as for NikA, an *E. coli* periplasmic nickel-protein (15)or human glyceraldehyde-3-phosphate dehydrogenase (16). Furthermore, a putative role for the protein Surf1 of *Paracoccus denitrificans* as a heme *a* chaperone involved in COX biogenesis was described (17). Recently, we described the heme binding protein HemW from *Lactococcus lactis* hypothesizing that HemW is involved in heme trafficking (13).

Here, we provide biochemical, genetic and biophysical evidences that the bacterial HemW proteins are heme chaperones for the insertion of heme *b* into enzymes of respiratory chains.

Results

E. coli *HemW has no coproporphyrinogen III dehydrogenase activity* in vitro *and* in vivo - *E. coli* HemN and HemW amino acid sequences are 33% identical but differ in two major features. *E. coli* HemN carries extra 46 N-terminal amino acid residues which have been proposed to be crucial for substrate binding (9). Moreover, the fourth cysteine of the HemN CX_3CX_2CXC motif is replaced by a phenylalanine in HemW. These differences are found in all HemW-like proteins (13). To investigate whether HemW carries coproporphyrinogen III dehydrogenase (CPDH) activity, it was first analyzed *in vitro*. For this purpose *E. coli* HemN and HemW were recombinantly produced and purified to apparent homogeneity. In contrast to HemN (18), *E. coli* HemW completely failed to catalyze the conversion of coproporphyrinogen III into protoporphorynogen IX. In a next step *in vivo* complementation experiments using the *E. coli* Δ*hemN* strain JKW3838 under anaerobic growth conditions were performed. Due to the presence of the oxygen-dependent coproporphyrinogen III oxidase HemF this mutant grew efficiently under aerobic conditions (data not shown). However, in the absence of oxygen a severe growth impairment was detected. Minimal remaining growth might result from fermentative energy generation or residual HemF activity. Clearly, *E. coli hemN* (pET3-hemN) complemented the Δ*hemN E. coli* strain to wildtype comparable growth, while *E. coli* pGEX*hemW* failed to restore anaerobic growth of the mutant (Fig.1). Both results clearly indicate that *E. coli* HemW does not harbor coproporphyrinogen III dehydrogenase activity as was also observed for *L. lactis* HemW (13).These results are in agreement with heme auxotrophy reported for a *Salmonella typhimurium hemF/hemN* double mutant carrying an intact *hemW*(19). In order to test if the deviating N-terminus and the missing fourth cysteine residue were responsible for the observed behavior we constructed a HemW F25C protein carrying the fourth cysteine and a HemW-HemN hybrid protein carrying the 46 N-terminal amino acids of HemN fused to HemW F25C. Nevertheless, HemWF25C+46N-term did not show any coproporphyrinogen III dehydrogenase activity *in vitro*. In agreement, no complementation of the *E. coli* Δ*hemN* strain under anaerobic conditions was observed with any other of the HemW variants. Obviously, additional structural elements are required for efficient HemN activity. Consequently, HemW is not an inactivated potential coproporphyrinogen III dehydrogenase.

E. coli *HemW binds a [4Fe-4S] cluster* - For the biochemical and biophysical characterization, *E. coli* HemW was produced as glutathione S-transferase (GST) fusion protein in *E. coli* BL21 DE3. After anaerobic chromatographic purification and removal of the GST tag by PreScission protease cleavage, an apparent homogenous protein was obtained. SDS-PAGE analysis revealed a single protein band after staining with Coomassie Blue (Fig. 2*A*). The protein had a relative molecular mass of ~ 45,000 ±5,000 which nicely corresponds to the calculated molecular mass for the HemW monomer of 42,584 Da. Approximately 12.5 mg of purified HemW were obtained per liter of culture. To elucidate if *E. coli* HemW coordinates an iron-sulfur cluster, the iron and sulfur contents of the protein were determined. For native, purified HemW, no obvious absorption around 410 - 425 nm was detectable in the UV/Vis absorption spectrum. Purified HemW exhibited 0.5 mol iron/0 mol sulfur per mol HemW and an A_{420}:A_{280} ratio of 0.04. Consequently, we decided for a reconstitution of the obviously labile [Fe-S] cluster via treatment of the protein with iron ammonium citrate and lithium sulfide. After reconstitution the iron and sulfur content of HemW increased to 3.8 mol iron/2.5 mol sulfur per mol HemW and an A_{420}:A_{280} ratio of 0.19. As a consequence, the typical absorbance for [Fe-S] clusters at 420 nm became clearly visible (Fig. 2*B*). To further characterize the cluster type of HemW, the iron-sulfur cluster of HemW was reconstituted with ^{57}Fe-ammonium ferric citrate and Mössbauer spectroscopy of ^{57}Fe reconstituted HemW was performed. Mössbauer spectra were recorded for samples containing HemW. Spectra without further addition revealed one dominant quadrupole doublet (83% of the total intensity) with an isomer shift (δ) of 0.49 mm/s and a quadrupole splitting parameter (ΔE_Q) of 1.00 mm/s, which are typical of $[4Fe\text{-}4S]^{2+}$ clusters (Fig. 2*C*, *dashed line*). Moreover, a second quadrupole doublet (17% of the total intensity) with an isomer shift (δ) of 1.48 mm/s and a quadrupole splitting parameter (ΔEQ) of 3.30 mm/s was detected (Fig. 2*C*, *dotted line*). The solid line in Figure 2 represents the superposition of the two quadrupole doublets. This spectrum is consistent with a coordination of the iron-sulfur cluster by three cysteine ligands and one potential N/O ligand. The three cysteine residues are likely the Cys^{16}, Cys^{20} and Cys^{23} of the CX_3CX_2C motif at the N-terminus of the protein sequence. The high isomer shift of the second quadrupole doublet excludes an orgin from [Fe-S] clusters, but reveals high-spin Fe(II) sites with six hard O- or N- ligands; the component is therefore assigned to adventitiously bound Fe(II) in the protein, presumably remaining from the reconstitution procedure. However, various attempts to reduce the $[4Fe\text{-}4S]^{2+}$ cluster with different electron donor systems (e.g. sodium dithionite, titanium III citrate, with redox mediators) for subsequent EPR analysis failed. In contrast, the [4Fe-4S] cluster of the related *E. coli* HemN could be reduced at such conditions (18) and employed for successful EPR measurements. Surprisingly, cyclic voltammetry measurements clearly indicated a redox transition of the iron-sulfur cluster of HemW at around -410 mV (Fig. 3). The potential of -410 mV is in the range of

values found for other radical SAM enzymes (20). At this redox potential both dithionite and titanium III citrate should serve as efficient electron donors for HemW. Obviously, electron donor compounds are prevented to access the [4Fe-4S] cluster for reduction, consequently no radical reaction can be initiated. A similar explanation has been suggested for the [Fe-S] cluster in succinate dehydrogenase subunit B, which appears to be inaccessible for oxidants and toxins (21).

The HemW [4Fe-4S]$^{2+}$ cluster promotes protein dimerization - To study the influence of the iron-sulfur cluster on the oligomerization state of HemW, experiments using size-exclusion chromatography of anaerobically purified and reconstituted HemW and of a HemW variant (C16S-C20S-C23S) lacking the [4Fe-4S] cluster were performed (Fig. 4). For the [4Fe-4S] cluster containing HemW, two fractions corresponding to monomeric (fraction 16) and dimeric protein (fraction 14) were detected (Fig. 4*A*). Calibration of the column revealed, that fraction 16 for the monomeric protein corresponded to a M_r of 45,000 ± 5000 and fraction 14 for the dimeric protein to a Mr of 87,000 ± 6000. Interestingly, an increased amount of iron-sulfur cluster was spectroscopically detected at 420 nm for the dimeric HemW species compared to the monomeric form (Fig. 4A, dashed line). Nevertheless, iron-sulfur clusters were also detected in monomeric HemW, which indicated a dynamic transition between monomeric and dimeric HemW. This transition between monomeric and dimeric proteins was tested by re-chromatography of the collected separated monomeric and dimeric HemWs in fraction 14 and fraction 16 on the gelfiltration column. We observed, that re-chromatography of the dimeric HemW in fraction 14 resulted again in two equal sized protein absorption peaks in fractions 14 and 16 (Fig. 4*C*). However, most iron sulfur cluster absorption was detected for the dimeric protein in fraction 14. Analogously, re-chromatography of monomeric protein in fraction 16 generated also two absorption maxima in fraction 14 and 16, however, with the bigger peak in fraction 16 representing the monomeric protein (Fig 4*D*). An analytical gelfiltration analysis of HemW without [Fe-S] cluster, caused by the replacement of cysteines 16, 20 and 23 to serines of the iron-sulfur cluster binding motif revealed only one single peak in fraction 16 corresponding to a monomeric protein (Fig. 4*B*). The C16S-C20S-C23S HemW variant was subjected to iron-sulfur cluster reconstitution experiment analogously to the wildtype protein prior these experiments, but remained iron-sulfur cluster free as determined spectroscopically and by iron and sulfur determinations. Obviously, an equilibrium exists between the monomeric and dimeric protein, however, formation of a dimeric HemW is favored by the incorporation of the iron-sulfur cluster.

E. coli *HemW binds SAM* - The amino acid sequence analysis of *E. coli* HemW clearly revealed two binding sites for S-denosyl-L-methionine (SAM) similar to the radical SAM enzyme HemN from *E. coli*. Overall, in *E. coli* HemN 19 amino acid residues are known from the crystal structure of the protein to coordinate 2 SAM molecules and 1 [4Fe-4S] cluster. Of the involved 19 HemN amino residues 11 (R184, G113, T114, C66, C62, C69, Q172, D209, Y56, G112, E145, clockwise around the binding site (Fig. S2) were found identical in HemW (R138, G67, T68, C20, C16, C23, Q126, D163, Y10, G66, E95) and 3 homologous (I211 in HemN– M165 in HemW, F240 – Y194, F68 – Y22), when the amino acid sequences of the proteins were aligned. Due to the low amino acid

sequence conservation at the C-terminus of both proteins, an aligment of 4 amino acid residues of HemN (A243, A242, F310, I329) did not match the corresponding residues of HemW. The region of HemN is involved in coproporphyrinogen III coordination and represents most likely the heme binding region of HemW. Only the cysteine (C71) and the residue aside (G70) used to clearly differentiate HemN from HemW proteins were found clear cut different (F25, D24). For experimentally studying SAM-binding of HemW, the purified reconstituted protein was incubated with ^{14}C-SAM and the mixture passed over a desalting column for the removal of non-incorporated free SAM. Protein-bound ^{14}C-SAM was subsequently quantified using liquid scintillation counting. The control experiment was carried out using BSA and ^{14}C-SAM. The HemW-^{14}C-SAM complex was eluted in the protein-containing fractions (Fig. 5*A, solid line, fractions 1-4*). Some free ^{14}C-SAM eluted in the later, small molecule fractions. In contrast all ^{14}C-SAM incubated with BSA eluted in the small molecules fraction (Fig. 5*A, dashed line, fractions 6-14*). Consequently, SAM binding to HemW was clearly demonstrated. The highly conserved structure of the SAM and [4Fe-4S]-cluster binding site suggested the presence of two SAM molecules. However, due to the unknown amount of already bound SAM in the tested HemW proteins and the unknown exchange rate between bound and unbound SAM, it was not possible to determine the stoichiometry of SAM binding to HemW.

Analysis of the SAM cleavage capacity of HemW - The classical radical SAM enzyme chemistry requires the reduction of the [4Fe-4S] cluster, homolytic cleavage of the S–C(5') bond of SAM with the generation of the 5'-deoxyadensosyl radical. HemN usually requires its substrate coproporphyrinogen III for radical formation (10). However, in the absence of the substrate residual enzymatic SAM cleavage of usally less than 15% of the reaction without substrate was observed. To test HemW for full or residual SAM cleavage activity reconstituted HemW protein was incubated with SAM and with and without heme as potential substrate under reducing conditions. The disappearance of SAM with the parallel formation of deoxyadenosine was monitored by HPLC analysis (Fig 5*B, solid line*). The same experiment was performed as control with purified HemN in absence and presence of substrate (Fig. 5*B, dashed and dotted line*). In this case under tested conditions *E. coli* HemN revealed full SAM cleavage activity in the presence of the substrate coproporphyrinogen III (Fig. 5*B, dotted line*) and less than 5% of its SAM cleavage activity without substrate (Fig. 5*B, dashed line*). Comparable residual SAM cleavage capacity was observed for HemW with the addition (Fig. 5*B, solid line*) and without the addition of heme (not shown). Clearly, *E. coli* HemW revealed only the residual SAM cleavage activity comparable to HemN without substrate (Fig. 5B).

HemW is a heme binding protein - Previous studies with the HemW homolog from *L. lactis* revealed heme binding to the protein (13). In order to test for heme binding of *E. coli* HemW and determine its specificity, the purified HemW protein and heme were incubated anaerobically overnight and analyzed spectrophotometrically (Fig. 6A, dotted line). As control the employed protein solution and free heme were analyzed in parallel. HemW showed only the typical protein absorption at 280 nm and little absorption for the iron-sulfur cluster (Fig 6*A, solid line*). Free heme showed the typical spectrum with peaks around 400 nm and 580 nm (Fig 6*A, dashed line*). The HemW-heme complex revealed a broad absorption peak between 380 and

420 nm besides the protein absorbance at 280 nm (Fig 6*A*, *dotted line*). In order to determine the specificity of heme binding, all three samples (HemW, heme, HemW-heme complex) were subjected to extensive dialysis overnight and subsequent spectroscopic analyses. While the spectrum for HemW did not change (Fig 6*B*, *solid line*) and the spectrum for the HemW-heme complex only lost its little increase around 400 nm (Fig 6*B*, *dotted line*), all free heme was gone (Fig 6*B*, *dashed line*). Identical results were obtained for the dialyzed and Superdex 200 gelfiltrated HemW-heme complex (data not shown). Interestingly, reduction ot the HemW-heme complex resulted in an increase of absorption at 424 nm generating a Soret band and further absorption peaks at 531 nm and 559 nm (Fig 6*c*, *dashed line*). In contrast, free reduced heme shows an absorption peak at around 400 nm. These results demonstrate the specificity of HemW-heme interaction.

For the further analysis of the nature and stoichiometry of HemW-heme interaction, complexes were analyzed via SDS PAGE with heme staining and acidified butanone extraction. HemW and equimolar amounts of heme were incubated overnight and subjected in duplicate to SDS PAGE analyses. Subsequently, one half of the gel was stained with Coomassie Brillant Blue for detection of separated proteins (Fig. 7*A*, *lane 1*), while the proteins on the second half of the gel were blotted onto a nitrocellulose membrane for heme staining. The detection of the HemW bound heme was based on its intrinsic peroxidase activity by incubation with the ECL reagent (Fig. 7*A*, *lane 2*). The observed heme staining of *E. coli* HemW indicated stably bound heme. In order to obtain further evidence for the possible covalent nature of heme binding, butanone extraction experiments were performed which can result either in release of non-covalently linked heme in the organic phase or still bound, covalently linked heme in the aqueous phase (22). Cytochrome *c* was used as a positive control clearly indicating the presence of covalently bound heme in the aqueous phase (Fig. *7B, middle picture*). Hemoglobin with non-covalently bound heme was used as negative control. Here, almost all heme was extracted in the upper organic phase (Fig. 7*B*, *right picture*). Butanone extraction of HemW incubated with heme revealed a completely clear upper phase and a slightly brownish lower phase (Fig. 7*B*, *left picture*). The presence of HemW derived heme in the lower aqueous phase indicated covalently bound heme. Even though our experiment pointed towards covalently bound heme, strong binding of the heme in a tight hydrophobic pocket resistant to SDS and butanone treatment can not be excluded. Subsequently, the heme staining assay was used to identify the binding stoichiometry of HemW and heme. For this purpose, a solution of 10 µM HemW (Fig 7*C*, *lanes 1 to 5*) was titrated with heme in increasing amounts from 5 µM concentration to 25 µM (Fig 7*C*, *lanes 6 to 10*). The subsequent heme staining revealed an increase of the heme bound to HemW up to a heme concentration of 10 µM indicating that apparent saturation of the signal occurred after addition of equimolar amounts of heme (Fig 7*C*, *lanes 6 to 10*). Alternatively, heme binding stoichiometry by HemW was determined spectroscopically by using 20 µM native HemW which was titrated with increasing amounts of heme. Measurements of the optical density at 416 nm revealed a heme-binding saturation at 20 µM (Fig. 7D). These results clearly indicate a specific binding with a stoichiometry of one molecule heme per HemW monomer.

Heme binding is independent of the presence of the iron-sulfur cluster - Aerobically prepared HemW without iron-sulfur cluster was binding heme as efficient as anaerobically prepared HemW

with the cluster. Similiarly, the HemW triple mutant (HemW-C16SC20SC23S) also bound heme with high efficiency. In agreement, the Mössbauer spectrum of HemW supplemented with non-enriched heme (natural isotope distribution, only 2.2 % ^{57}Fe) showed the same spectrum and identical fit parameters as HemW without further additions. The presence of heme only slightly changed the observed redox potential of the iron-sulfur-cluster of around -410 mV (Fig. 3). These results demonstrate that the iron sulfur cluster was not affected by heme binding. Vice versa, the iron sulfur cluster did not influence heme binding by HemW. Moreover the presence of SAM did not change heme binding of HemW.

Respiratory nitrate reductase and bacterioferritin are interaction partners of HemW - In order to determine specific targets for the potential heme chaperone HemW multiple interaction partners were tested using the BACTH (Bacterial Adenylate Cyclase Two-Hybrid) system in *Pseudomonas aeruginosa*. The *P. aeruginosa* system was employed because high background noise levels were observed for similar experiments in *E. coli*, which obscured the results. In this study, the hemoenzymes bacterial ferritin BfrA, bacterioferritin BfrB, catalase KatA, the last enzyme of heme biosynthesis ferrochelatase HemH and the heme containing subunit of the respiratory nitrate reductase NarI were analyzed for their interaction with HemW. The choices for testing BfrA and B as well KatA and Ferrochelatase HemH are obvious, since all proteins are heme binding/storing enzymes. The consecutive ß-galactosidase assays reveled the highest Miller units for the combination of HemW with NarI indicating their strong affinity. Furthermore, HemW interacted with BfrA and BfrB but not with HemH or KatA. In agreement, in the inverse experiment HemH and KatA neither interacted with HemW (Fig. 8).

HemW transfers heme to heme-depleted quinol-nitrate oxidoreductase NarGHI - The strongest interaction of HemW was found with the heme containing subunit NarI of the respiratory nitrate oxidoreductase NarGHI. Under anaerobic conditions and the presence of nitrate *E. coli* utilizes this enzyme for energy generation by replacing oxygen with nitrate as terminal electron acceptor. This respiratory complex has the ability to use all three natural quinones for energy generation (23,24). For our approach, ubiquinol served as electron donor and the membrane-anchored subunit NarI provides the quinol binding and oxidation site. Two low-spin hemes (b_H and b_L) involved in the electron transfer from quinols to the subunit NarG are coordinated by NarI (25). The presence of both hemes was demonstrated to be essential for the oxidation of quinols and the overall activity of NarGHI as deduced from analysis of NarI variants having lost either heme b_H or b_L (26). In order to unambiguously identify HemW as true heme chaperone, heme transfer analyses from HemW to the quinol nitrate oxidoreductase NarGHI from *E. coli* were performed. Thus, Nar-enriched membrane vesicles from *E. coli* wildtype MC4100 and the heme deficient *E. coli* Δ*hemA* were prepared. The absence of heme in the heme-depleted membrane vesicles due to the Δ*hemA* gene mutation was obvious by the visible change in color of the membrane preparation (Fig. 9*B*) and the corresponding UV-Vis spectra (Fig. 9*A*). First, the enzymatic activity of heme-depleted nitrate oxidoreductase was tested spectrophotometrically using a quinol analog as electron donor (27). A classical spectrophotometric activity assay for the nitrate reductase NarGHI was used. It is based on the absorption changes of the employed artificial electron donor the

menaquinol analog 2-methyl-1,4-naphtoquinol (menadiol). The oxidation from menadiol to menadione during the reduction of nitrate to nitrite was followed spectroscopically at 260 nm. As mentioned above, only heme containing NarGHI can catalyze menadiol oxidation in the presence of nitrate. Results of the heme transfer to the NarGHI are summarized in box plots in figure 9*C*. Membrane vesicles prepared from *E. coli* wildtype MC4100 served as positive control in this experiment (Fig. 9*C, lane A*). Activity assays of membrane vesicles containing heme-depleted quinol nitrate oxidoreductase revealed only low residual enzymatic activity (Fig. 9*C, lane B*). However, addition of HemW pre-incubated with heme lead to a significant nitrate reductase activity (Fig. 9*C, lane C*). Addition of NADH further increased the observed enzyme activity (Fig. 9*C, lane D*). Over 50% of the potentially possible nitrate reductase acitivity was restored. Full restoration might be hampered by the possible instablility of the heme free apo enzyme compared to the holo nitrate reductase. In the negative controls, *E. coli* Δ*hemA* mutant membrane vesicles with the addition of solely heme or apo HemW exhibited residual background activity identical to the results of the heme-free nitrate reductase (Fig. 9*C, lanes E and F*). Similiarly, the combination of heme, HemW and NADH did not react with the used nitrate reductase substrate (Fig. 9*C, lane H*). SAM did not influence the heme trasnsfer reaction. To analyze the influence of the [4Fe-4S] cluster on heme transfer, a HemW triple mutant (HemW-C16SC20SC23S) lacking the cluster was tested. The activity of NarGHI was not restored by the triple mutant HemW (Fig. 9*C, lane G*), while the heme binding behavior of the mutant enzyme was comparable to wildtype HemW. The observed catalytic activity of the nitrate oxidoreductase in the membrane vesicles prepared from the heme-deficient *E. coli* Δ*hemA* mutant after addition of heme-loaded HemW clearly indicates sucessful heme transfer from HemW to the heme-requiring NarI subunit. These results support the function of HemW as heme chaperone.

Slight growth phenotype of the E. coli hemW *mutant* – In the light of the heme chaperone function of HemW for the respiratory nitrate reductase NarGHI, growth experiments with wildtype and a *hemW* mutant under anaerobic, nitrate respiratory conditions with the non-fermentable carbon source glycerol were performed. Under tested growth condition the *hemW* mutant showed a slight, but highly reproducible growth phenotype (Fig. 1*B, blue line*). In the absence of nitrate almost no growth was observed. The observed growth of the *hemW* mutant indicated the presence of intact nitrate reductase and a second heme inserting system supplementing for the inactivated HemW. Backup systems for essential functions were observed in *E. coli* for catalases, ribonucleotide reductases, and pyruvate kinases, to name a few.

Human HemW homologue RSAD1 binds heme - RSAD1 from *Homo sapiens* (30 % amino acid sequence identity, 50 % homology) was analyzed for heme binding via its recombinant production in *E. coli*, affinity purification and heme staining (Fig. 10*A*). Clearly, heme bound strongly to human RSAD1. Additionally, a typical absorption spectrum was also recorded for the *H. sapiens* RSAD1-heme complex (Fig. 10*B*). Alltogether, the experiments for human RSAD1 confirmed the results for bacterial HemW suggesting the ubiquitous function of HemW/RSAD1 as heme chaperone.

Discussion

HemW protein inserts heme into proteins of different functions in respiration. Genes encoding HemW/RSAD1 are found in the

genomes of almost all organisms (bacteria, archaea, plants, animals) with the noticable exception of fungi. The presence of *hemW* genes nicely correlates with the utilization of heme-dependent aerobic and anaerobic respiration. Consequently, *hemW* is even found in organisms which employ heme taken up from the environment for this process like *Lactococci* (13). In contrast, strict fermentative organisms like *Clostridia*, deficient in heme biosynthesis and heme uptake due to the absence of classical heme-dependent respiratory processes, are also lacking HemW. How does this radical SAM protein based heme chaperone work? As shown in the model in figure 11 heme can be derived from the biosynthesis and heme import. Interestingly, no stable complex formation between HemW and ferrochelatase (HemH), the last enzyme of the heme biosynthesis, was observed (28). However, heme from HemW was found interacting with BfrA and BfrB. In 1999, Hassett and coworkers reported that *P. aeruginosa* catalase A (KatA) requires bacterial ferritin A (BfrA) for full activity. They proposed that BfrA does not only store iron for the incorporation into heme, but also the necessary prosthetic heme group of KatA (29). Consequently, BfrA could function as a heme transporter between HemH, the last enzyme of heme biosynthesis and the heme- accepting protein KatA.

Recently, a radical SAM protein (ChuW) with heme degradating activity from *E. coli* was described. ChuW utilizes a radical-based mechanism for the heme ring opening and the methylation of the resulting open chain tetrapyrrole (30). *E. coli* ChuW has an amino acid sequence identity of 28 % to *E. coli* HemW. However, almost all identical amino acid residues are part of the N-terminal radical SAM element of both proteins. No common heme binding domain was detected.

Based on these observations and data of this contribution a model for HemW as depicted in figure 11 was deduced. Heme produced in heme biosynthesis gets transferred via bacterioferritin to HemW where it is covalently bound. In the presence of the [4Fe-4S] cluster HemW dimerizes, gets located to the membrane and interacts with its target NarI. Transfer of the heme requires an intact [4Fe-4S] cluster and might involve radical chemistry. The exact mechanism of the NADH stimulation of heme transfer remains to be determined Finally, the human RSAD1 protein was found to bind heme tightly, indicating the general importance of HemW/RSAD1 enzyme family for the heme insertion into cellular proteins. Future experiments will focus on the biochemistry of the heme release from HemW to target proteins and the role of the radical chemistry in it.

Experimental Procedures

Primers, strains and plasmids

The primers, strains and plasmids used in this study are listed in table S1.

Cloning, Expression and Purification of E. coli hemW

The *hemW* gene was PCR-amplified from *E. coli* genomic DNA using the primers *hemW*$_{E.c.}$-pGEX - for and *hemW*$_{E.c.}$-pGEX - rev harboring a *BamHI* and a *XhoI*-restriction site (underlined), respectively. The PCR product of 1137 bp was cloned into the respectively restricted vector pGEX-6P-1 according to the manufacturer's instructions, yielding the plasmid pGEX-HemW$_{E.c.}$. The vector encoded HemW with an N-terminal glutathione S-transferase tag (GST-tag) and a cleavage site for PreScission protease (GE Healthcare, München, Germany). GST-HemW was produced in *E. coli* BL21 (DE3) with the help of the plasmid pGEX-HemW$_{E.c.}$. Cultures of 2 liters were grown aerobically in LB and 100 mg/ml ampicillin at 200 rpm and

37 °C. The *hemW* gene expression was induced at an attenuance of 578 nm of 0.6 by the addition of 0.5 mM isopropyl-ß-D-thiogalactoside (IPTG), and cultivation was continued overnight at 17 °C and 200 rpm. Cells were harvested by centrifugation at 4000 x *g* for 15 min at 4 °C. All following steps occurred under strict anaerobic conditions at 20 °C. For HemW purification, cells were resuspended in 10 ml buffer 1 (140 mM NaCl, 2.7 mM KCl, 10 mM Na_2HPO_4, 1.8 mM KH_2PO_4, 5% glycerol, 1 mM DTT, pH 7.4) and cells were disrupted by a single passage through a French Press at 19,200 p.s.i.. Cell debris and insoluble proteins were removed by centrifugation for 60 min at 25000 x *g* and 4 °C. The soluble protein fraction was loaded onto a glutathione sepharose column (Machery-Nagel, Düren, Germany). HemW was liberated from the column by cleavage of the GST tag overnight with PreScission protease (GE Healthcare, München, Germany) according to the manufacturer's instructions. HemW-containing fractions were eluted, pooled and concentrated by ultrafiltration using an Amicon membrane with a 30 kDa molecular mass cut-off (Merck Millipore, Billerica, USA). Protein concentrations were determined with the colorimetric assay using the Bradford reagent with bovine serum albumin as standard according to manufacturer´s instructions. (Sigma-Aldrich, Taufkirchen, Germany) The triple mutant *hemW*C16SC20SC23S was constructed using the Q5® site-directed mutagenesis kit (New England Biolabs, Frankfurt, Germany) according to manufacturer's instructions. Successful construction of mutations was confirmed by DNA sequencing of the complete *hemW* gene variant. Production and purification of the HemW variant was performed analogously to wildtype HemW.

Absorption Spectroscopy

UV-visible absorption spectra of HemW and HemW-heme complexes were recorded on a Jasco V-650 spectrophotometer (Jasco, Gross-Umstadt, Germany) in buffer 1, using the same buffer as a blank. The recording wavelengths were from 250 - 600 nm. 10 mg Heme were dissolved in 1 ml 0.1 M NaOH and incubated at RT for 1h. After addition of 1 ml Tris-HCl (1 M, pH 7.6) the solution was centrifuged at 12.100 x *g* at RT for 10 min. The supernatant was filtered from insoluble residues and the concentration was determined at the OD_{385nm} X/58.44=x * 500= x mmol/l

In vitro *Iron-Sulfur Cluster Analysis*

The *in vitro* reconstitution of [Fe-S] clusters was performed as described previously (31). After reconstitution of the [Fe-S] cluster the excess of iron and sulfide was removed by centrifugation at 12.100 x *g* and 4 °C and subsequent passage of the protein solution through a NAP-25 column (GE Healthcare, München, Germany) according to the manufacturer's instructions. The iron content of purified HemW was determined according to a protocol described elsewhere (32). After denaturation of the protein with 1 M perchloric acid, bathophenanthroline was used as the chelating reagent. The sulfur content was determined as previously described (33).

Mössbauer Spectroscopy

The final HemW concentration employed for Mössbauer spectroscopy analysis of *E. coli* HemW was 350 µM. Sample preparation was performed under strict anaerobic conditions. The iron-sulfur cluster of HemW was reconstituted with ^{57}Fe-ammonium ferric citrate. For the sample containing HemW supplemented with heme an equimolar ratio of heme to HemW was added, and the mixture incubated overnight at 20 °C. The solutions were transferred to 350 µl Mössbauer cups and frozen in liquid nitrogen. Mössbauer spectra were recorded on a spectrometer with alternating constant acceleration of the γ-source. The minimum experimental line width was 0.24 mms^{-1} (full width at

half-height). The sample temperature was maintained constant in an Oxford Instruments Variox cryostat, whereas the ^{57}Co/Rh source (1.8 GBq) was kept at room temperature. Isomer shifts are quoted relative to iron metal at 300 K.

Cyclic Voltammetry

Cyclic voltammetry measurements were performed using an Ametek Versastat 3. The measurements were carried out in a self-made anaerobic three-electrode electrochemical cell flushed with nitrogen. As the reference, a silver/silver-chloride electrode was used (3 mol l^{-1} KCl). All potentials in the text and figures are given *vs.* NHE (+210 mV). A platinum wire was used as the counter electrode, with glassy carbon as the working electrode. Before each measurement the platinum wire was annealed in a natural gas flame and the glassy carbon electrode was pretreated in nitric acid, neutralized, polished with 0.05 µm alumina and annealed again in a natural gas flame. For each experiment 20 cycles were recorded. The potential slightly drifted only over the first 10 cycles and stabilized thereafter. In this work, only the stabilized potential is discussed. The cycles were recorded with a scan rate of 1 V s^{-1}. All electrochemical experiments were carried out at ambient temperature in a 100 µl drop. Samples contained 120 µM HemW, 120 µM heme or 500 µM S-adenosylmethionine (Sigma-Aldrich, Taufkirchen, Germany) in diverse combinations. Samples were prepared under anaerobic conditions in a glove box (Coy Laboratories) and transferred into HPLC vials before injecting into the CV chamber directly on the glassy carbon electrode.

SAM binding and cleavage analyses

The SAM-binding assays were performed as described previously (34). For this purpose 100 µM purified HemW or BSA were incubated 0.5 µCi S-[carboxyl-^{14}C] SAM (1.48-2.22 GBq/mmol, 0.1 mCi/ml) at 25 °C for 1h. Mixtures were separated via chromatography through am illustraTM NAPTM-5 desaltiung column (GE Healthcared, Freiburg, Germany). Fractions of 200 µl were collected and analyzed by liquid scintillation counting (Perkin Elmer, Waltham, USA).

For SAM cleavage, 25 µM purified HemW (free or loaded with heme) were incubated with 0.6 mM sodium dithionite as potential electron donor and 0.6 mM SAM overnight at 17 °C under anaerobic conditions. Reactions were stopped by adding 5 % formic acid. For HPLC analysis the samples were centrifuged at 16.100 x g für 10 min. HPLC analysis was performed as described previously (20). In detail, for the separation of 5'-deoxyadenosine from SAM a hypercarb column (Thermo Fisher Scientific, Waltham, USA) at a JASCO 2000 system (JASCO, Groß-Umstadt, Germany) with a flow rate of 0.2 ml/min was used at room teperature. A 5 ml gradient of 0.1 % TFA in H_2O and 0.08 % TFA in acetonitrile was applied. SAM and 5'-deoxyadenosine were detected at 254 nm. Appropriate markers were used to calibrate the column.

Determination of the Native Molecular Mass

An Äkta purifier system for gel permeation chromatography with a Superdex 200 HR 10/300 column was used (GE Healthcare, München, Germany). The column was equilibrated using buffer 1 and calibrated using carbonic anhydrase (Mr = 9,000), bovine serum albumin (Mr = 66,200), yeast alcohol dehydrogenase (Mr = 150,000) and β-amylase (Mr = 200,000) as marker proteins. A sample containing purified recombinant HemW was chromatographed under identical conditions with a flow rate of 0.25 ml/min under anaerobic conditions.

Heme binding assays

One mg heme was dissolved in 100 µl of 100 mM NaOH and thoroughly mixed (34). After 30 min 100 µl 1 M Tris, pH 7.4 was added. The solution was

centrifuged at 4 °C for 10 min at 12,100 x *g*. The concentration was determined using ε_{385} = 58.44 (mM cm)$^{-1}$. HemW was incubated with an equimolar concentration of heme under anaerobic conditions at 20 °C overnight and the formed complex was used for further analyses including spectroscopy, heme staining, and the *in vitro* transfer reaction to NarGHI.

For detection of the stable HemW-heme complex, the heme-complexed protein was separated via SDS PAGE followed by electrophoretic transfer to an Amersham Hybond-ECL nitrocellulose membrane (GE Healthcare, München, Germany). After three washing steps with buffer 2 (137 mM NaCl, 2.7 mM KCl, 10 mM Na_2HPO_4, 1.8 mM KH_2PO_4) the nitrocellulose membrane was incubated for 5 min with Amersham™ ECL™ Prime Western Blotting Detection Reagent (GE Healthcare, München, Germany). Heme was detected by its intrinsic peroxidase activity (35) with a CCD camera. Acidic butanone extraction was performed as described elsewhere (22,36).

Protein/Protein Interaction studies using Bacterial Adenylate Cyclase Two-hybrid system (BACTH)

The BACTH (Bacterial Adenylate Cyclase Two-hybrid) System Kit (Euromedex, Souffelweyersheim, Frankreich) was used to analyse the interaction between *P. aeruginosa* HemW and selected partner proteins from the same bacterium (BfrA, KatA, HemH, BfrB and NarI). Corresponding genes were amplified by PCR using *P. aeruginosa* genomic DNA as template DNA. Used primers were listed in table S1. Genes were integrated into plasmids pKT25, pKNT25, pUT18 and pUT18C, respectively (Euromedex, Souffelweyersheim, Frankreich). For the detection of the *in vivo* interaction, selected plasmids, encoding the genes for the proteins of interest, were cotransformed into the reporter strain *E. coli* BTH101 cells and washed after transformation twice with M63 buffer (2g $(NH_4)_2SO_4$, 13.6 g KH_2PO_4, 0.5 mg $FeSO_4 \cdot 7\ H_2O$, 1 ml 1 M $MgSO_4 \cdot 7\ H_2O$,
10 ml 20 % maltose, 2 ml 0.05% thiamin, pH 7.0). Colonies were selected on M63 agar plates containing ampicillin (100 µg/ml) or kanamycin (50 µg/ml) or streptomycin (100 µg/ml), 5-bromo-4-chloro-3-indolyl-β-D-galactopyranoside (X-Gal) (40 µg/ml) and IPTG (0,5 mM). Incubation for 4 to 8 days was at 30 °C. β-Galactosidase assays were performed accordingly to the method of Miller (37). For this purpose, blue *E. coli* BTH101 colonies were used to inoculate LB medium supplemented with 100 µg/ml ampicillin and 50 µg/ml kanamycin. Hundred µl bacterial suspension were centrifuged at 4.400 x g for 5 min at 4 °C. The resulting pellet was resuspended in 900 µl of Z buffer (60 mM $Na_2PO_4 \cdot 7\ H_2O$, 40 mM $NaH_2PO_4 \cdot H_2O$, 10 mM KCl,
1 mM $MgSO_4 \cdot 7\ H_2O$,
50 mM ß-mercaptoethanol) and the cell density was measured at 600 nm. Afterwards, one drop of 0,1 % SDS and chloroform were added. The sample was incubated for 5 min at 30 °C and 300 rpm. The reaction was started by adding 200 µl ONPG (o-Nitrophenyl-β-D-galactopyranosid, 4 mg/ml) dissolved in 100 mM phosphate buffer (60 mM $Na_2HPO_4 \cdot 7H_2O$ and 40 mM $NaH_2PO_4 \cdot H_2O$, pH 7.0). The suspension was mixed and incubated at 30 °C. The reaction was terminated by adding 500 µl 1 M Na_2CO_3. A centrifugation step for 5 min at 12700 x g removed cell debris and chloroform. Optical densities were recorded at 420 nm and 550 nm. Miller Units (MU) were calculated MU 1000 x $(OD_{420} - (1.75 \times OD_{550}) / (T_R \times V \times OD_{600})$, where T_R stands for time of the reaction in minutes, V for volume of culture used in the assay in ml. The units indicate the change in A_{420}/min/ml of cells/OD_{600}.

Heme transfer to heme-free quinol nitrate oxidoreductase NarGHI

The heme auxotroph *hemA* strain SHSP18 (38) was transformed with the pVA700 plasmid (39) allowing overproduction of the NarGHI complex. Isolation of the transformants was performed on LB-agar plate supplemented with 40 mM glucose and 150 µM δ-aminolevulinic acid. The following steps were performed simultaneously for the *hemA* strain SHSP18 and the wild type strain *E. coli* MC4100 (40) both transformed with the pVA700 plasmid. An LB overnight culture supplemented with glucose (40 mM), sodium formate (12.5 mM), sodium selenite (2 µM), sodium molybdate (2 µM) and phosphate buffer (100 mM, pH 6.8) was inoculated with a single colony of the corresponding strains. The production culture was then inoculated with this overnight culture to an initial OD_{600} of 0.05 in the identical medium and incubated for 24 hours at 37 °C. The grown cells were pelleted by centrifugation and kept at -20 °C until use. Cells were resuspended in 50 mM MOPS buffer, 1 mM $MgCl_2$, pH 7.2 and broken by two passages through a French press at 1100 p.s.i. Intact cells and cell debris were removed by a centrifugation at 14000 x g. Membrane vesicles were obtained after ultracentrifugation at 40,000 x g for 90 minutes and kept at -80 °C until use. The amount of NarGHI in the various preparations was determined via immuno-electrophoresis. The various membrane vesicle preparations from the wildtype strain had 85 to 95 mg/ml total protein with 5.6 to 7.9 mg/ml (6.5 - 8.3 %) NarGHI protein, while preparation from the *hemA* mutant yielded 60 to 106 mg/ml total protein with 3.6 to 5.8 mg/ml (5.5 - 6.0%) NarGHI protein. Standard deviation between 3 to 5 % were observed. All measurements were performed with equal amounts NarGHI (4 µg) and 1.5 µM purified HemW/HemW-C16SC20SC23S. For the assay 20 mM 2-methyl-1,4-naphtoquinol (menadiol) as electron donor, 5 mM NADH, 1.5 µM mM free heme, 2 mM nitrate as electron acceptor were added where indicated. A quartz cell with 1.4 ml volume was used. The assay was performed under strict anaerobic conditions at 30 °C. The activity of *E. coli* quinol nitrate oxidoreductase was measured spectrophotometrically as outlined before (27). The changes in absorption of the ubiquinol analog 2-ethyl-4-naphtoquinol (menadiol) caused by oxidation was measured at 260 nm. A quartz cell with 1.4 ml volume was used. The assay was performed under strict anaerobic conditions at 30 °C. One unit of quinol nitrate oxidoreductase activity is the amount of nitrate oxidoreductase catalyzing the production of 1 µmol of menadione per min.

Acknowledgements - This work was supported by grants from the Deutsche Forschungsgemeinschaft (Forschergruppe FOR1220 PROTRAIN). We especially thank Léa Sylvi for excellent technical assistance and Gunhild Layer for critical reading of the manuscript.

Conflict of Interest - The authors declare that they have no conflicts of interest with the contents of this article.

Author Contribution - VH, SK, TM, SB, KM, PS performed the experiments, FA and AM prepared the NarGHI heme-depleted membrane vesicles, EB and WL performed the Mössbauer spectroscopy with HemW, KK, MB provided the ^{57}Fe, PS provided electrochemical analyses; and VH, MJ and DJ designed the experiments and wrote the manuscript.

REFERENCES

1. Frey, P. A., Hegeman, A. D., and Ruzicka, F. J. (2008) The Radical SAM Superfamily. *Crit Rev Biochem Mol Biol* **43**, 63-88
2. Landgraf, B. J., McCarthy, E. L., and Booker, S. J. (2016) Radical S-Adenosylmethionine Enzymes in Human Health and Disease. *Annu Rev Biochem* **85**, 485-514
3. Wang, J., Woldring, R. P., Roman-Melendez, G. D., McClain, A. M., Alzua, B. R., and Marsh, E. N. (2014) Recent advances in radical SAM enzymology: new structures and mechanisms. *ACS Chem Biol* **9**, 1929-1938
4. Byer, A. S., Shepard, E. M., Peters, J. W., and Broderick, J. B. (2015) Radical S-adenosyl-L-methionine chemistry in the synthesis of hydrogenase and nitrogenase metal cofactors. *J Biol Chem* **290**, 3987-3994
5. Frey, P. A., and Reed, G. H. (2011) Pyridoxal-5'-phosphate as the catalyst for radical isomerization in reactions of PLP-dependent aminomutases. *Biochim Biophys Acta* **1814**, 1548-1557
6. Mehta, A. P., Abdelwahed, S. H., Mahanta, N., Fedoseyenko, D., Philmus, B., Cooper, L. E., Liu, Y., Jhulki, I., Ealick, S. E., and Begley, T. P. (2015) Radical S-adenosylmethionine (SAM) enzymes in cofactor biosynthesis: a treasure trove of complex organic radical rearrangement reactions. *J Biol Chem* **290**, 3980-3986
7. Sanyal, I., Cohen, G., and Flint, D. H. (1994) Biotin synthase: purification, characterization as a [2Fe-2S]cluster protein, and in vitro activity of the *Escherichia coli bioB* gene product. *Biochemistry* **33**, 3625-3631
8. Helbig, K. J., and Beard, M. R. (2014) The role of viperin in the innate antiviral response. *J Mol Biol* **426**, 1210-1219
9. Layer, G., Moser, J., Heinz, D. W., Jahn, D., and Schubert, W. D. (2003) Crystal structure of coproporphyrinogen III oxidase reveals cofactor geometry of Radical SAM enzymes. *EMBO J* **22**, 6214-6224
10. Layer, G., Verfurth, K., Mahlitz, E., and Jahn, D. (2002) Oxygen-independent coproporphyrinogen-III oxidase HemN from *Escherichia coli*. *J Biol Chem* **277**, 34136-34142
11. Layer, G., Grage, K., Teschner, T., Schunemann, V., Breckau, D., Masoumi, A., Jahn, M., Heathcote, P., Trautwein, A. X., and Jahn, D. (2005) Radical S-adenosylmethionine enzyme coproporphyrinogen III oxidase HemN: functional features of the [4Fe-4S] cluster and the two bound S-adenosyl-L-methionines. *J Biol Chem* **280**, 29038-29046
12. Dailey, H. A., Gerdes, S., Dailey, T. A., Burch, J. S., and Phillips, J. D. (2015) Noncanonical coproporphyrin-dependent bacterial heme biosynthesis pathway that does not use protoporphyrin. *Proc Natl Acad Sci U S A* **112**, 2210-2215
13. Abicht, H. K., Martinez, J., Layer, G., Jahn, D., and Solioz, M. (2012) *Lactococcus lactis* HemW (HemN) is a haem-

binding protein with a putative role in haem trafficking. *Biochem J* **442**, 335-343
14. Kranz, R. G., Richard-Fogal, C., Taylor, J. S., and Frawley, E. R. (2009) Cytochrome c biogenesis: mechanisms for covalent modifications and trafficking of heme and for heme-iron redox control. *Microbiol Mol Biol Rev* **73**, 510-528, Table of Contents
15. Shepherd, M., Heath, M. D., and Poole, R. K. (2007) NikA binds heme: a new role for an *Escherichia coli* periplasmic nickel-binding protein. *Biochemistry* **46**, 5030-5037
16. Hannibal, L., Collins, D., Brassard, J., Chakravarti, R., Vempati, R., Dorlet, P., Santolini, J., Dawson, J. H., and Stuehr, D. J. (2012) Heme binding properties of glyceraldehyde-3-phosphate dehydrogenase. *Biochemistry* **51**, 8514-8529
17. Hannappel, A., Bundschuh, F. A., and Ludwig, B. (2012) Role of Surf1 in heme recruitment for bacterial COX biogenesis. *Biochim Biophys Acta* **1817**, 928-937
18. Layer, G., Pierik, A. J., Trost, M., Rigby, S. E., Leech, H. K., Grage, K., Breckau, D., Astner, I., Jansch, L., Heathcote, P., Warren, M. J., Heinz, D. W., and Jahn, D. (2006) The substrate radical of *Escherichia coli* oxygen-independent coproporphyrinogen III oxidase HemN. *J Biol Chem* **281**, 15727-15734
19. Xu, K., Delling, J., and Elliott, T. (1992) The genes required for heme synthesis in *Salmonella typhimurium* include those encoding alternative functions for aerobic and anaerobic coproporphyrinogen oxidation. *J Bacteriol* **174**, 3953-3963
20. Kuehner, M., Schweyen, P., Hoffmann, M., Ramos, J. V., Reijerse, E. J., Lubitz, W., Broering, M., and Layer, G. (2016) The auxiliary [4Fe-4S] cluster of the Radical SAM heme synthase from *Methanosarcina barkeri* is involved in electron transfer. *Chemical Science* **7**, 4633-4643
21. Rouault, T. A. (2015) Mammalian iron-sulphur proteins: novel insights into biogenesis and function. *Nat Rev Mol Cell Biol* **16**, 45-55
22. Teale, F. W. (1959) Cleavage of the haem-protein link by acid methylethylketone. *Biochim Biophys Acta* **35**, 543
23. Rendon, J., Pilet, E., Fahs, Z., Seduk, F., Sylvi, L., Hajj Chehade, M., Pierrel, F., Guigliarelli, B., Magalon, A., and Grimaldi, S. (2015) Demethylmenaquinol is a substrate of *Escherichia coli* nitrate reductase A (NarGHI) and forms a stable semiquinone intermediate at the NarGHI quinol oxidation site. *Biochim Biophys Acta* **1847**, 739-747
24. Unden, G., Steinmetz, P. A., and Degreif-Dunnwald, P. (2014) The Aerobic and Anaerobic Respiratory Chain of *Escherichia coli* and *Salmonella enterica*: Enzymes and Energetics. *EcoSal Plus* **6**
25. Bertero, M. G., Rothery, R. A., Palak, M., Hou, C., Lim, D., Blasco, F., Weiner, J. H., and Strynadka, N. C. (2003) Insights into the respiratory electron transfer pathway from the

structure of nitrate reductase A. *Nat Struct Biol* **10**, 681-687
26. Magalon, A., Lemesle-Meunier, D., Rothery, R. A., Frixon, C., Weiner, J. H., and Blasco, F. (1997) Heme axial ligation by the highly conserved His residues in helix II of cytochrome *b* (NarI) of *Escherichia coli* nitrate reductase A. *J Biol Chem* **272**, 25652-25658
27. Lanciano, P., Magalon, A., Bertrand, P., Guigliarelli, B., and Grimaldi, S. (2007) High-stability semiquinone intermediate in nitrate reductase A (NarGHI) from *Escherichia coli* is located in a quinol oxidation site close to heme bD. *Biochemistry* **46**, 5323-5329
28. Dailey, H. A., Dailey, T. A., Gerdes, S., Jahn, D., Jahn, M., O'Brian, M. R., and Warren, M. J. (2017) Prokaryotic Heme Biosynthesis: Multiple Pathways to a Common Essential Product. *Microbiol Mol Biol Rev* **81**
29. Ma, J. F., Ochsner, U. A., Klotz, M. G., Nanayakkara, V. K., Howell, M. L., Johnson, Z., Posey, J. E., Vasil, M. L., Monaco, J. J., and Hassett, D. J. (1999) Bacterioferritin A modulates catalase A (KatA) activity and resistance to hydrogen peroxide in *Pseudomonas aeruginosa. J Bacteriol* **181**, 3730-3742
30. LaMattina, J. W., Nix, D. B., and Lanzilotta, W. N. (2016) Radical new paradigm for heme degradation in *Escherichia coli* O157:H7. *Proc Natl Acad Sci U S A* **113**, 12138-12143
31. Fluhe, L., Knappe, T. A., Gattner, M. J., Schafer, A., Burghaus, O., Linne, U., and Marahiel, M. A. (2012) The radical SAM enzyme AlbA catalyzes thioether bond formation in subtilosin A. *Nat Chem Biol* **8**, 350-357
32. Fish, W. W. (1988) Rapid colorimetric micromethod for the quantitation of complexed iron in biological samples. *Methods Enzymol* **158**, 357-364
33. Beinert, H. (1983) Semi-micro methods for analysis of labile sulfide and of labile sulfide plus sulfane sulfur in unusually stable iron-sulfur proteins. *Anal Biochem* **131**, 373-378
34. Storbeck, S., Walther, J., Muller, J., Parmar, V., Schiebel, H. M., Kemken, D., Dulcks, T., Warren, M. J., and Layer, G. (2009) The *Pseudomonas aeruginosa nirE* gene encodes the S-adenosyl-L-methionine-dependent uroporphyrinogen III methyltransferase required for heme d(1) biosynthesis. *FEBS J* **276**, 5973-5982
35. Owens, C. P., Du, J., Dawson, J. H., and Goulding, C. W. (2012) Characterization of heme ligation properties of Rv0203, a secreted heme binding protein involved in *Mycobacterium tuberculosis* heme uptake. *Biochemistry* **51**, 1518-1531
36. Vargas, C., McEwan, A. G., and Downie, J. A. (1993) Detection of *c*-type cytochromes using enhanced chemiluminescence. *Anal Biochem* **209**, 323-326
37. Griffith, K. L., and Wolf, R. E., Jr. (2002) Measuring beta-galactosidase activity in bacteria: cell growth, permeabilization, and enzyme assays in 96-well arrays. *Biochem Biophys Res Commun* **290**, 397-402
38. Sasarman, A., Surdeanu, M., Szegli, G., Horodniceanu, T.,

Greceanu, V., and Dumitrescu, A. (1968) Hemin-deficient mutants of *Escherichia coli* K-12. *J Bacteriol* **96**, 570-572

39. Guigliarelli, B., Magalon, A., Asso, M., Bertrand, P., Frixon, C., Giordano, G., and Blasco, F. (1996) Complete coordination of the four Fe-S centers of the beta subunit from *Escherichia coli* nitrate reductase. Physiological, biochemical, and EPR characterization of site-directed mutants lacking the highest or lowest potential [4Fe-4S] clusters. *Biochemistry* **35**, 4828-4836
40. Peters, J. E., Thate, T. E., and Craig, N. L. (2003) Definition of the *Escherichia coli* MC4100 genome by use of a DNA array. *J Bacteriol* **185**, 2017-2021

FIGURE LEGENDS

FIGURE 1. Growth behavior of *E. coli hemN* and *hemW* mutants. A. *E. coli hemW* does not encode a coproporphyrinogen III dehydrogenase. Cells were grown anaerobically at 37 °C in LB medium containing 10 mM $NaNO_3$ and no antibiotics in tightly sealed anaerobic flasks. Changes in optical density at 578 nm were followed spectroscopically. Values for each strain are averages of three independent experiments with three parallel cultures. The growth of wildtype BW25113 (red), *E. coli* Δ*hemN* (green), Δ*hemN* with pET-3a-*hemN* (*E. coli hemN*) (orange) Δ*hemN* with pGEX*hemW*F25C (blue) and Δ*hemN* with pGEX*hemW*F25C+46N-term (purple) were compared. B. Slight growth phenotype of the *E. coli hemW* mutant. The anaerobic growth in M9 minimal medium supplemented with 5 mM KNO_3 and glycerol as non-fermentable carbon source was compared. Without KNO_3 almost no growth was observed. Growth of wildtype plus KNO_3 *E. coli* BW25113 (red solid line) and *E. coli* JW2922 (Δ*hemW*) (blue solid line) and the growth without KNO_3 of *E. coli* BW25113 (red dashed line) and *E. coli* JW2922 (Δ*hemW*) (blue dashed line) were compared. Changes in optical density at 578 nm were followed spectroscopically. Values for each strain are averages of six independent experiments with three parallel cultures.

FIGURE 3. Redox potential of the HemW bound [4Fe-4S] cluster. Cyclic voltammograms of HemW (black), buffer (red) and the resulting difference of HemW and buffer (blue). A redox potential of ~ 410 mV was deduced.

FIGURE 4. Influence of the Iron-sulfur cluster on the oligomeric state of HemW. Analytical gel permeation chromatography analyses of HemW (panels A, C,D) and the HemW-C16SC20SC23S variant (panel B) were performed using a Superdex® 200 10/300 GL column on an ÄKTApurifier system (GE Healthcare, Buckinghamshire, UK) with a flow rate of 0.5 ml/min. Protein absorption was followed at 280 nm (solid line) and iron-sulfur cluster absorption at 420 nm (dashed line). Fourty µM of anaerobically prepared and iron-sulfur-reconstituted HemW and of the triple mutant were chromatographed. The separated protein peaks of the HemW (A) in fractions 14 and 16 were individually collected and re-chromatographed. The re-run of fraction 14 is shown in C and of fraction 16 in panel D. Apart from monomeric (16) and dimeric HemW (14) detected during the re-chromatography shown in panels C and D, an additional shoulder peak was detected in fraction 13, most likely due to protein aggregation resulting from the concentration of HemW prior to the second chromatography.

FIGURE 5. SAM binding and SAM-cleavage by HemW. A: SAM-binding assay**.** 100 µM HemW were incubated with radioactive 0.5 µCi ^{14}C-SAM and fractionated via a desalting column. The radioactive fractions were analyzed using liquid scintillation counting. Solid line: HemW + ^{14}C-SAM; dashed line: BSA + ^{14}C-SAM. B: The SAM cleavage assays were performed for 25 µM *E. coli* HemW (solid line) supplemented with heme, 25 µM *E. coli* HemN without substrate (dashed line) and 25 µM *E. coli* HemN with its substrate coproporphyrinogen III (dotted line). After addition of 0.6 mM dithionite as potential electron donor, 0.6 mM SAM was added and the mixture was incubated. The reaction was stopped with formic acid. Samples were chromatographically separated on a hypercarb column with appropriate marker substances. SAM (indicated with a dot) and formed 5´-deoxyadenosine (indicated with a star) were detected at 254 nm. Background controls without protein

or BSA did not yield the 5´-deoxyadenosine specific peak. HemN in the presence of substrate revealed full SAM cleavage. Without substrate 5% residual SAM cleavage was observed for HemN. HemW with heme revealed comparable residual SAM cleavage activity.

FIGURE 6: Spectroscopic characterization of HemW heme binding. Shown are UV-Vis spectra from 250 to 700 nm. A: spectra of 20 µM HemW (solid line) 20 µM HemW after binding of 20 µM heme (dotted line). The dashed line shows the spectrum of 20 µM free heme. B: spectra of 20 µM HemW (solid line), HemW plus bound heme (dotted line) and free heme, all after extensive dialysis (dashed line). Free heme was completely removed after dialysis, while HemW and the stable HemW-heme complex remained. C: spectra of the 20 µM HemW-heme complex after dialysis (solid line) and after subsequent addition of 1 mM DTT (dotted line). To emphasize the changes at the wavelength 500 to 650 nm, this part of the spectra was enlarged.

FIGURE 7. One molecule HemW covalently binds one molecule heme. A: Twenty-five µM *E. coli* HemW were incubated with equimolar amount of heme. After SDS-PAGE separated proteins were either stained with Coomassie Brillant Blue (A1) or plotted onto a PVDF membrane. The peroxidase activity of heme is detectable based on the reaction with ECL reagent (A2); M, marker with proteins of known relative molecular masses. B: For butanone extraction, 25 µM of either HemW, or cytochrome *c*, or hemoglobin were incubated with 15 µM heme overnight. Afterwards the pH was adjusted to pH 1.5 with 10 % HCl. Ice-cold 2-butanone was added and carefully mixed. The heme bound to protein found in the lower aqueous phase indicated the covalently binding of heme to HemW (B, left tube). Butanone extraction from cytochrome *c* with covalently bound heme (horse heart, 1 mg/ml) served as a positive control (B, middle tube) and hemoglobin with non-covalently bound heme served as negative control (B, right tube). C: Heme stoichiometry of HemW binding. For heme staining, purified *E. coli* HemW (10 µM) was titrated with increasing amounts of heme (5 µM, 10 µM, 15 µM, 20 µM and 25 µM. The SDS-PAGE was stained with Coomassie Brillant Blue for protein visualization (lanes 1-5) and the blotted membrane with ECL reagent for bound heme (lanes 5-10). M: marker with proteins of known relative molecular masses. For spectroscopically determination of heme binding, 20 µM HemW was incubated with different amounts of heme. D: Titration curve for the determination of the stoichiometry of HemW and heme. Absorption was measured at 416 nm and plotted against increasing concentrations of heme. The intersection of the two linear slopes indicates the saturation of heme at approximately 20 M heme. Binding of one mol heme per mol of HemW monomer was concluded.

FIGURE 8. Identification of HemW protein interaction partner using a bacterial two hybrid system. Shown are the resulting ß-galactosidase activities in Miller units for the testing of the following bait-prey pairs: HemW-BfrA with pUT18C-*hemW*/pKT25-*bfrA* (1), HemW-HemH with pUT18C-*hemW*/pKT25-*hemH* (2), HemW-KatA with pUT18C-*hemW*/pKT25-*katA* (3), HemW-BfrB with pKT25-*hemW*/pUT18C-*bfrB* (4), HemW-NarI with pUT18C-*hemW*/pKNT25-*narI* (5), HemH-BfrB with pUT18C-*hemH*/pKT25-*bfrB* (6). pKNT25/pUT18 served as negative control (7) and pKT25-zip/pUT18C-zip as positive control (8).

FIGURE 9. HemW mediated heme transfer to the nitrate oxidoreductase NarGHI. A: Comparative spectroscopic analysis of prepared membrane vesicles from *E. coli* wild type MC4100 and the corresponding *E. coli* ΔhemA mutant. The recorded absorption spectrum at around 425 nm indicated the absence of bound heme cofactor in NarGHI produced by *E. coli* Δ*hemA* mutant (dashed line) in contrast to the spectrum recorded for the identical membrane vesicle preparation from wildtype *E. coli*. B: The decolorization of the prepared membrane vesicles (left tube wildtype, right tube Δ*hemA* mutant) due to the depletion of heme is optically visible. C: Enzyme assays were performed with membrane vesicles isolated from *E. coli* MC4100/pVA700 overexpressing *narGHJI* (labelled MC4100) and membrane vesicles with overproduced heme-depleted nitrate oxidoreductase isolated from *E. coli* Δ*hemA*/pVA700 (labeled Δ*hemA* SHSP18). The heme-depleted nitrate oxidoreductase was incubated with: HemW-heme (C), HemW-heme+NADH (D), [4Fe-4S] cluster less HemW-C16S-C20S-C23S-heme (G) and as negative controls solely with heme (E) or HemW (F) or HemW and NADH (H), respectively. 20 mM 2-methyl-1,4-naphtoquinol (menadiol) served as electron donor, 2 mM nitrate as electon acceptor, 5 mM NADH and 1.5 mM free heme were used where indicated. The range between -1 and 18 µmol/min*ml is shown.

FIGURE 10. Heme binding of HemW (RSAD1) from humans. A: For heme staining, purified RSAD1/HemW proteins of *Homo sapiens* (lanes 1, 3) and *E. coli* (lanes 2, 4) were incubated with heme overnight and separated via SDS PAGE. The proteins were stained with Instant*Blue*™ (Expedeon Inc., San Diego, USA) (lanes 1, 2) or blotted onto nitrocellulose membrane with subsequent ECL treatment for heme staining (lanes 3, 4). A marker indicated the relative molecular mass of the separated proteins. B: UV-Vis spectra of RSAD1 of *Homo sapiens* incubated with heme overnight. An absorption maximum at 410 nm indicated heme binding. Peaks at 531 nm and 556 nm were typical for incorporated heme.

FIGURE 11. Working model of *E. coli* HemW. Heme from heme biosynthesis gets transferred via bacterioferritin (Bfr, gray) as a carrier to the heme chaperone HemW (orange). Dimerized, the [4Fe-4S] cluster-containing HemW localizes to the membrane where it interacts with its target protein NarI (yellow), a subunit of the respiratory nitrate reductase NarGHI. After heme incorporation into apo-NarI, the holo-NarGHI catalyzes the reduction of nitrate to nitrite. PPO is protoporphyrinogen IX oxidase, FC (HemH) is ferrochelatase.

FIGURES

FIGURE 1

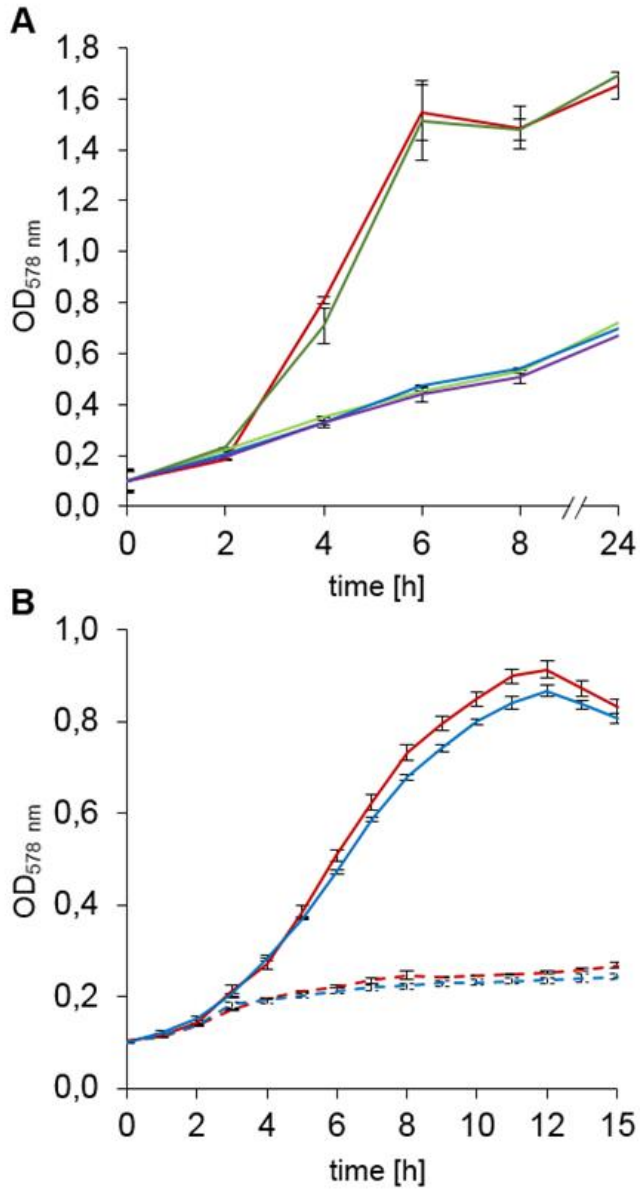

FIGURE 2

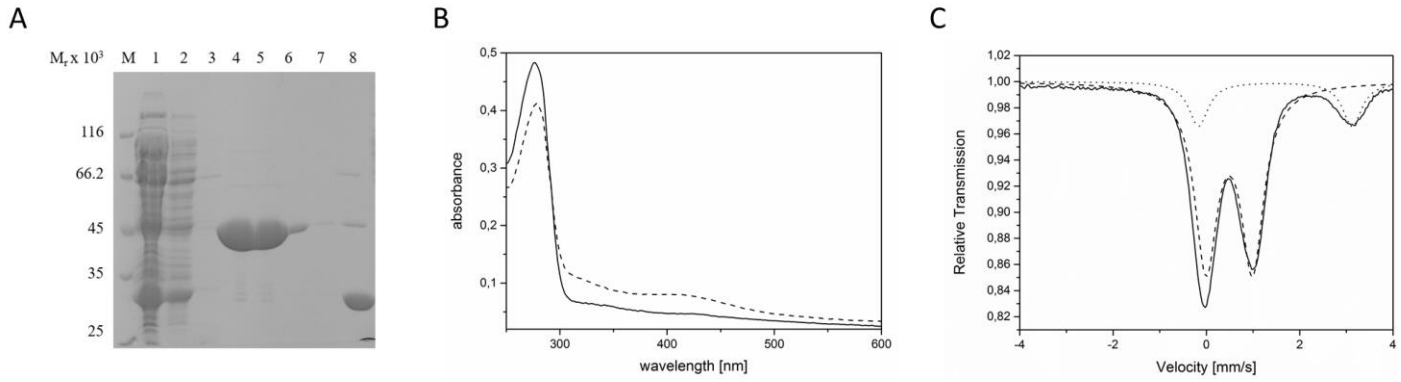
A
M_r x 10^3 M 1 2 3 4 5 6 7 8
116
66.2
45
35
25
B
absorbance
wavelength [nm]
C
Relative Transmission
Velocity [mm/s]

FIGURE 3

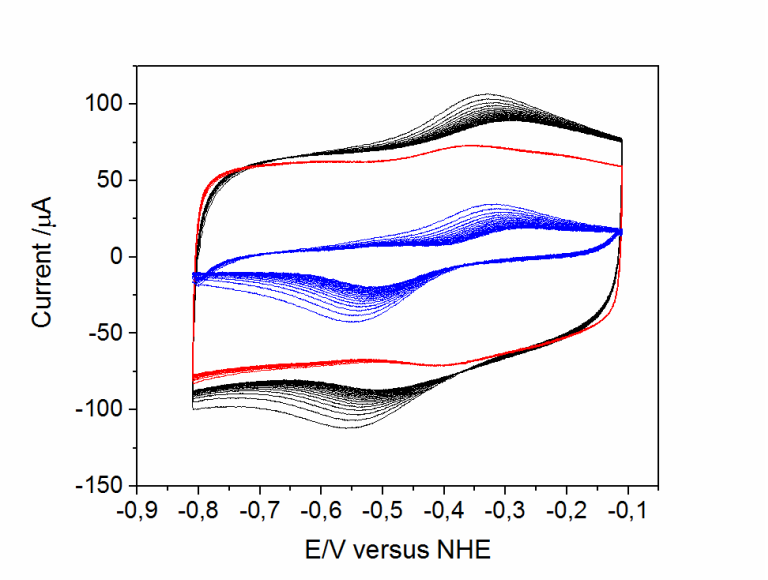
100
50
0
-50
-100
-150
Current /µA
-0,9
-0,8
-0,7
-0,6
-0,5
-0,4
-0,3
-0,2
-0,1
E/V versus NHE

FIGURE 4

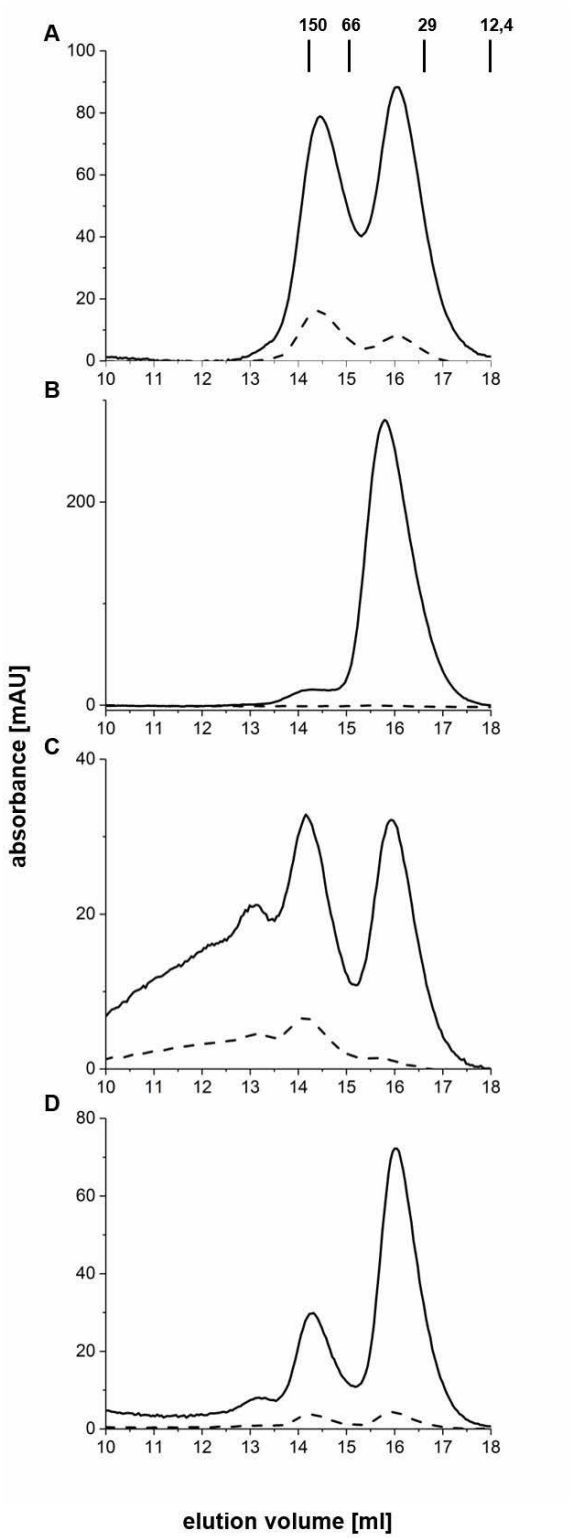

FIGURE 5

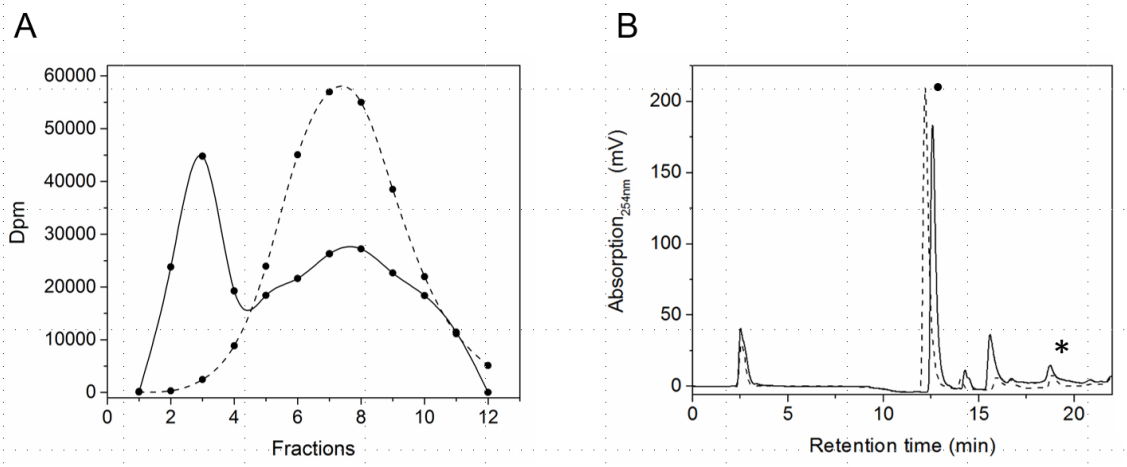
A
Dpm
60000
50000
40000
30000
20000
10000
0
0
2
4
6
8
10
12
Fractions
B
Absorption254nm (mV)
200
150
100
50
0
0
5
10
15
20
Retention time (min)
*

FIGURE 6

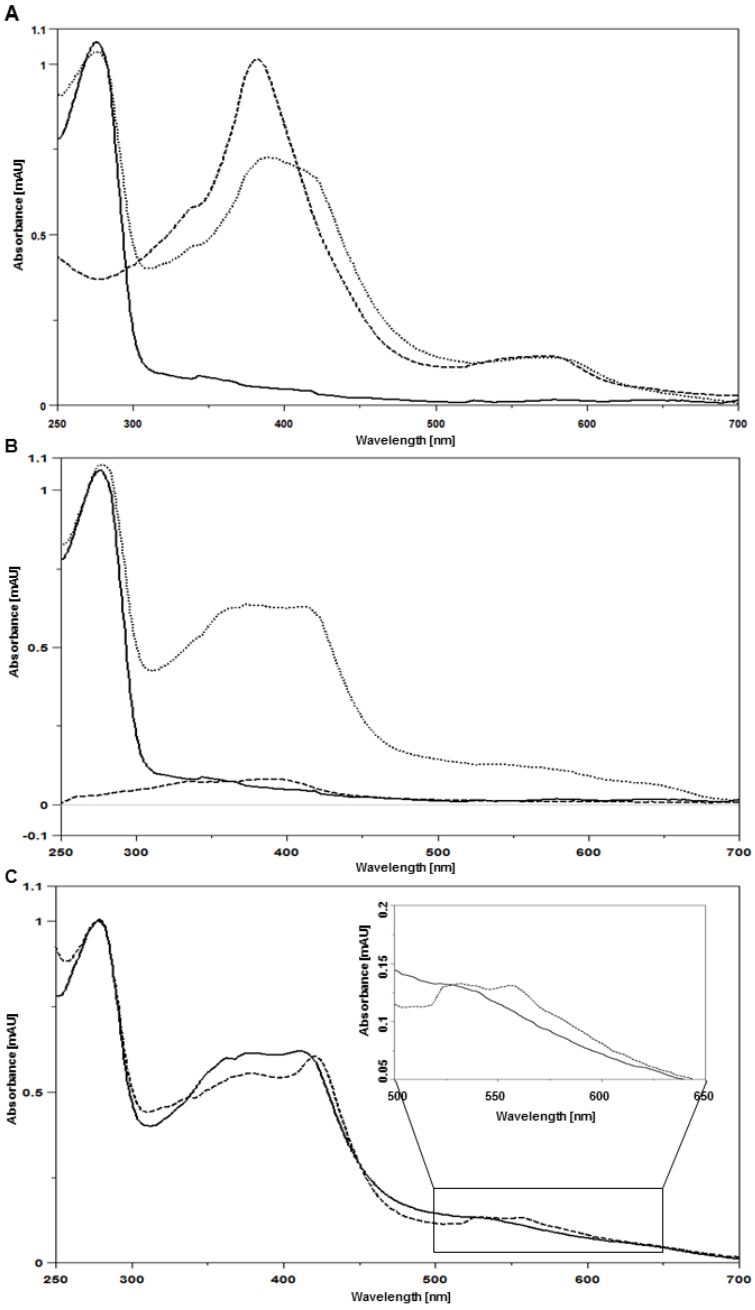
A
Absorbance [mAU]
Wavelength [nm]
B
Absorbance [mAU]
Wavelength [nm]
C
Absorbance [mAU]
Wavelength [nm]
Absorbance [mAU]
Wavelength [nm]

FIGURE 7

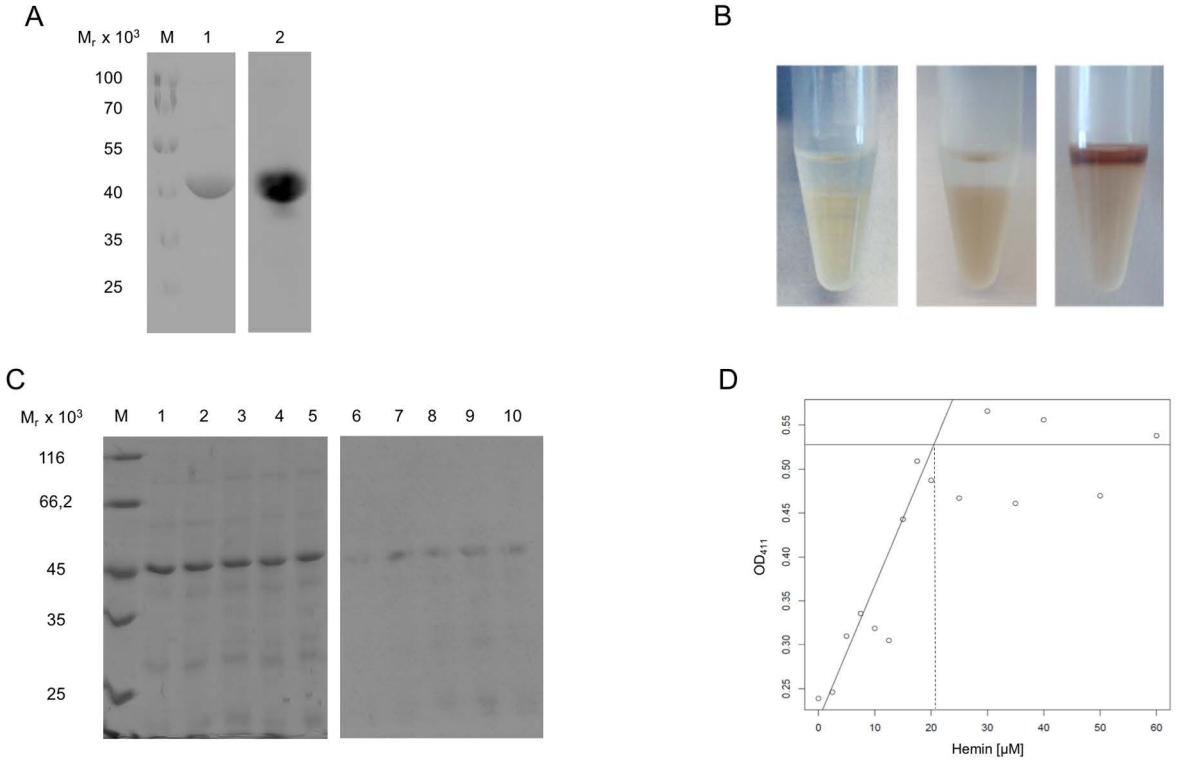
A
Mr x 10³
M
1
2
100
70
55
40
35
25
B
C
Mr x 10³
M
1
2
3
4
5
6
7
8
9
10
116
66,2
45
35
25
D
OD411
0.25
0.30
0.35
0.40
0.45
0.50
0.55
0
10
20
30
40
50
60
Hemin [μM]

FIGURE 8

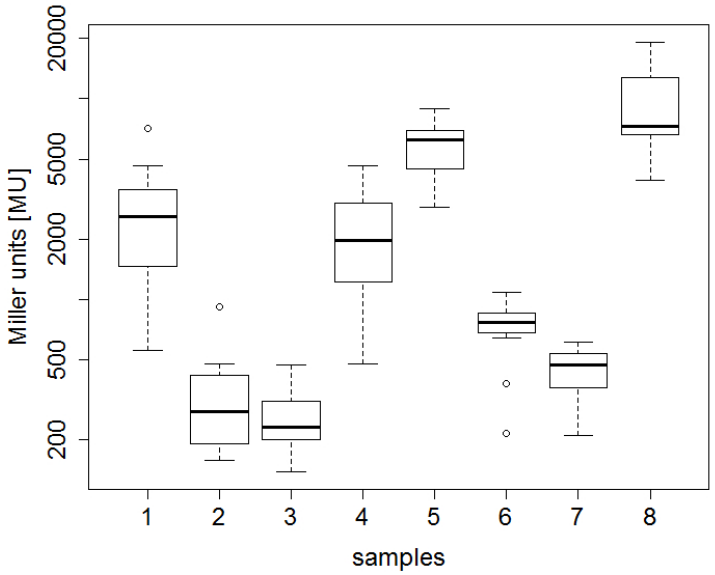

FIGURE 9

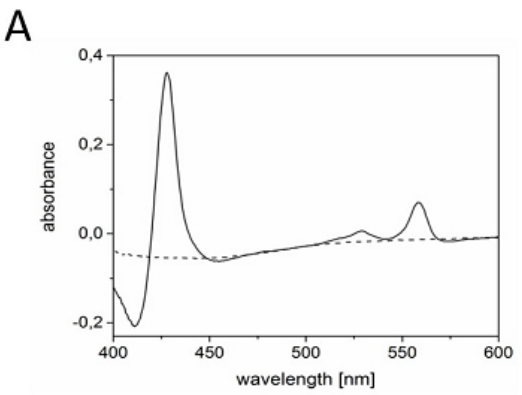

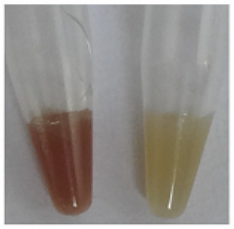

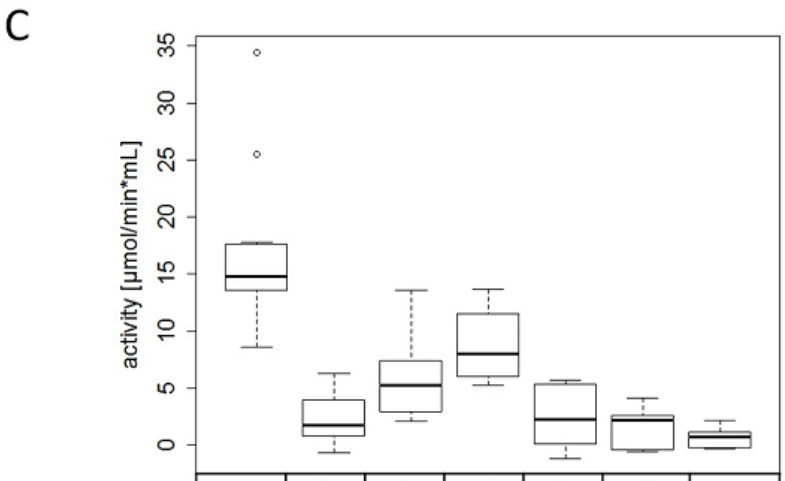

	A	B	C	D	E	F	G
MC4100	+	-	-	-	-	-	-
Δ*hemA* SHSP18	-	+	+	+	+	+	+
HemW	-	-	+	+	-	+	-
Hemin	-	-	+	+	+	-	+
NADH	-	-	-	+	-	-	-
HemW-C16S-C20S-C23S	-	-	-	-	-	-	+

FIGURE 10

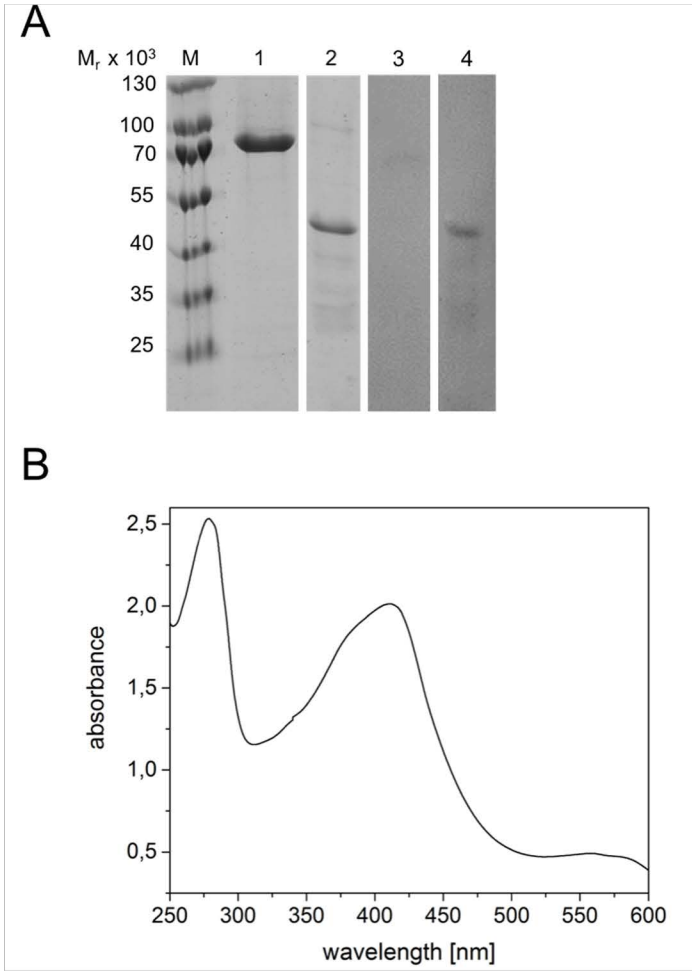
A
Mr x 10³
M
1
2
3
4
130
100
70
55
40
35
25
B
absorbance
2,5
2,0
1,5
1,0
0,5
250
300
350
400
450
500
550
600
wavelength [nm]

FIGURE 11

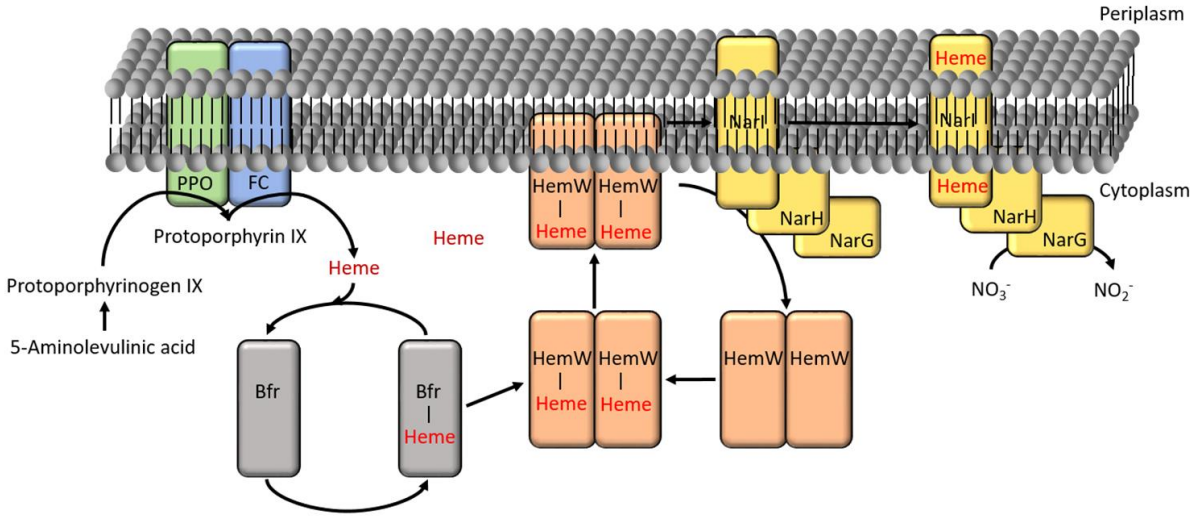
Periplasm
Heme
NarI
NarI
PPO
FC
HemW
Heme
HemW
Heme
Heme
NarH
NarG
Heme
NarH
NarG
Cytoplasm
Protoporphyrin IX
Heme
Heme
Protoporphyrinogen IX
5-Aminolevulinic acid
Bfr
Bfr
Heme
HemW
Heme
HemW
Heme
HemW
HemW
NO_3^-
NO_2^-